

This document is confidential and is proprietary to the American Chemical Society and its authors. Do not copy or disclose without written permission. If you have received this item in error, notify the sender and delete all copies.

**Yttrium-Enriched Phosphate Glass-Ceramic Microspheres for
Bone Cancer Radiotherapy Treatment.**

Journal:	ACS Omega
Manuscript ID	ao-2024-02825v.R3
Manuscript Type:	Article
Date Submitted by the Author:	n/a
Complete List of Authors:	Milborne, Ben; University of Nottingham, Arjuna, Andi; University of Nottingham Islam, Md Towhidul; University of Nottingham Arafat, Abul; University of Wolverhampton Layfield, Robert; University of Nottingham, School of Biomedical Sceinces Thompson, Alexander; University of Nottingham Ahmed, Ifty; University of Nottingham, School of Mechanical, Materials and Manufacturing Engineering,

SCHOLARONE™
Manuscripts

1
2
3
4
5
6
7
8
9
10
11
12
13
14
15
16
17
18
19
20
21
22
23
24
25
26
27
28
29
30
31
32
33
34
35
36
37
38
39
40
41
42
43
44
45
46
47
48
49
50
51
52
53
54
55
56
57
58
59
60

Yttrium-Enriched Phosphate Glass-Ceramic Microspheres for Bone Cancer Radiotherapy Treatment

Ben Milborne^a, Andi Arjuna^{a,c}, Md Towhidul Islam^a, Abul Arafat^b, Robert Layfield^c, Alexander Thompson^d and Ifty Ahmed^{a*}

^aAdvanced Materials Research Group, Faculty of Engineering, University of Nottingham, Nottingham, NG7 2RD, UK. benjamin.milborne@nottingham.ac.uk (B.M.); andi.arjuna@nottingham.ac.uk (A.A.); Towhid.Islam@nottingham.ac.uk (T.I.); ifty.ahmed@nottingham.ac.uk (I.A.); ^bSchool of Engineering, University of Wolverhampton, Telford Innovation Campus, Telford, TF2 9NT, UK. a.arafat@wlv.ac.uk (A.Ab.); ^cSchool of Life Sciences, Faculty of Medicine and Health Sciences, University of Nottingham, Nottingham, NG7 2UH, UK; robert.layfield@nottingham.ac.uk (R.L.); ^dBiodiscovery Institute, Division of Cancer and Stem Cells, University of Nottingham, Nottingham, NG7 2RD, UK; alex.thompson@nottingham.ac.uk (A.T.); ^e Faculty of Pharmacy, Hasanuddin University, Makassar, 90245, Indonesia; *Correspondence: ifty.ahmed@nottingham.ac.uk

KEYWORDS: Yttrium, glass, radiotherapy, bone cancer, bone repair, tissue regeneration

ABSTRACT: This study presents the development and characterisation of high yttrium-content phosphate-based glass-ceramic microspheres for potential applications in bone cancer radiotherapy treatment. The microspheres produced via flame spheroidisation, followed by sieving, revealed a lack of aggregation and a narrow size distribution (45 – 125 µm) achieved across different yttrium oxide to glass ratio samples. EDX analysis showed a significant increase in yttrium content within the microspheres with increasing yttrium oxide to glass ratio samples, ranging from approximately 1 mol % to 39 mol % for 10Y to 50Y microspheres, respectively. Concurrently, a proportional decrease in phosphate, calcium, and magnesium content was observed. Further EDX mapping showed homogenous distribution of all elements throughout the microspheres, indicating uniform composition. XRD profiles confirmed the amorphous nature of the starting P40 glass microspheres, whilst yttrium-containing microspheres exhibited crystalline peaks corresponding to cubic and hexagonal Y₂O₃ and Y(PO₄) phases, indicating formation of glass-ceramic materials. Ion release studies revealed reduction of all ion release rates from yttrium-containing microspheres compared to P40 microspheres. The pH of the surrounding media was also stable at approximately pH 7 over time, highlighting the chemical durability of the microspheres' produced. *In vitro* cytocompatibility studies demonstrated both indirect and direct cell culture methods showed favourable cellular responses. The metabolic and alkaline phosphatase (ALP) activity assays indicated comparable or enhanced cell responses on yttrium-containing microspheres compared to the initial P40 glass microspheres. Overall, these findings showed that significantly high yttrium-content phosphate glass-ceramic microspheres could be produced as versatile biomaterials offering potential applications for combined bone cancer radiotherapy treatment and bone regeneration.

Introduction

Internal radiation therapy is a cancer treatment method that involves positioning radioactive sources inside the body, typically near or directly within a tumor. [1]. This treatment can be particularly effective against cancers, especially where the response to chemotherapy is poor or when external beam radiotherapy is not possible due to the location of the cancerous tissue [2]. Effective treatment requires delivering radiation that maximizes the dose to malignant cancer cells while minimising exposure to adjacent healthy cells [3]. One strategy that has successfully been used to deliver internal radiotherapy is the use of radionuclide doped microspheres [4].

Various biomaterials have been employed to deliver specific radionuclides that emit alpha, beta or gamma radiation for internal radiation therapy. Beta-emitting (β) radionuclides are extensively employed owing to their capability to administer high radiation doses with adequate tissue penetration [5]. The selection of an appropriate radionuclide is guided by its

properties, ensuring the optimal delivery of the desired radiation dose over the necessary distance to maximize treatment efficacy for the targeted tissue or organ [6].

Yttrium 90 (⁹⁰Y) is a radionuclide that has been used to clinically deliver internal radiotherapy. Non-radioactive ⁸⁹Y is activated to the pure β -emitter ⁹⁰Y by neutron bombardment prior to implantation, with the resulting ⁹⁰Y having a half-life of 64.2 hours, a tissue penetration depth ranging from 2.5 -11 mm and the capability of delivering therapeutic doses of ionising radiation [7]. Currently two types of ⁹⁰Y containing microspheres are commercially available for use in Selective Internal Radiation Therapy (SIRT) (also known as radioembolisation) for the treatment of unresectable hepatocellular carcinoma [8]. SIR-Spheres (Sirtex Medical, Sydney, Australia) are resin-based microspheres comprised of a proprietary biocompatible microsphere coated with a cross-linked cation exchange polystyrene resin [9]. TheraSphere (Boston Scientific, United Kingdom) are alumina silicate glass

microspheres produced via traditional melt-quenching technique involving yttrium oxide (Y_2O_3), aluminium oxide and silicon dioxide, followed by flame-spheroidisation [10].

Glass microspheres are highly appealing for internal radiotherapy delivery, as the non-radioactive isotope can be integrated into the glass's chemical and physical structure during their manufacture [11]. Once the glass microspheres are manufactured, neutron activation occurs, which ensures an inherent safety benefit by minimizing radiation exposure during their fabrication. Once irradiated, the glass microspheres need to possess high chemical durability in order to prevent leaching of the radionuclide and irradiating the patient away from the target site. [12]. The time from neutron activation of the microspheres to their delivery in the clinic is also used to ensure administration of specific doses [13]. Despite this, significant decay of the microspheres radioactivity occurs before treatment has started due to the relatively short half-life of ^{90}Y [14].

The amount of Y_2O_3 that can be incorporated into the structure of silicate-based glasses is currently limited to around 18 mol% and requires a high temperature melting process, due to Y_2O_3 melting temperature of $2,425^\circ\text{C}$ [15]. Several studies in the literature have reported on the use of phosphate-based glasses as versatile vectors for internal radiotherapy due to their ability to encapsulate radionuclides, facilitating targeted radiation therapy while minimising damage to surrounding healthy tissues [16-18]. However, in phosphate-based glasses Y_2O_3 addition has been limited to around 5 mol% as further addition resulted in crystallisation of the glass, although Martin *et al.* incorporated approximately 31 mol% Y_2O_3 within yttrium alumino-phosphate glasses [19], [20]. To enhance therapeutic efficacy, there is a desire to increase the yttrium content within glass vectors, as the low concentration currently incorporated reduces the maximum dose of radiation, thereby necessitating a longer activation time through neutron bombardment to achieve the desired radiation dose levels.[21].

The biocompatibility and controlled release properties of certain phosphate-based glasses have meant they have also become valuable candidates for bone repair and regeneration applications [22]. Phosphate-glass microspheres have gathered significant research interest for their dual potential in serving as carriers for internal radiotherapy delivery while simultaneously facilitating bone repair. This dual functionality arises from their ability to encapsulate radionuclides for targeted therapy and to act as biocompatible scaffolds promoting bone regeneration, presenting a promising avenue for multifaceted medical applications.

This study reports on the processing and characterisation of high yttrium-content phosphate-based glass-ceramic microspheres for potential applications in delivering internal radiotherapy for the treatment of bone cancers. *In vitro* cytocompatibility studies have also been performed to assess the microspheres' ability to support cell growth and proliferation and to facilitate bone repair and regeneration to damage tissue following devastation due to bone cancer and its associated treatments.

Materials and Methodology

Glass fabrication

The P40 phosphate glass formulation ($40\text{P}_2\text{O}_5 \cdot 16\text{CaO} \cdot 24\text{MgO} \cdot 20\text{Na}_2\text{O}$ mol%) was prepared using the following precursors: sodium dihydrogen phosphate (NaH_2PO_4), calcium hydrogen phosphate (CaHPO_4), calcium carbonate (CaCO_3) and magnesium hydrogen phosphate trihydrate ($\text{MgHPO}_4 \cdot 3\text{H}_2\text{O}$) (Sigma Aldrich, UK). The precursors were accurately weighed based on the specified composition and thoroughly mixed before being heated in a 5% Au/Pt crucible at 350°C for 30 minutes. This initial heating phase aimed to dehydrate the samples and eliminate CO_2 . Subsequently, the mixture was melted at 1150°C with a heating rate of $10^\circ\text{C}/\text{min}$ and maintained at this temperature for 90 minutes. The resulting molten glass was quenched between two stainless steel plates at room temperature.

Microsphere manufacture

Microspheres were manufactured according to the method previously described in [42]. The P40 phosphate glass was ground using a Retsch PM100 milling machine and sieved into a size range of $45\text{--}63\text{ }\mu\text{m}$. For yttrium-containing microspheres, the glass was mixed with the corresponding ratio of yttrium (III) oxide (ACROS Organics, UK) using a Vortex-Genie 2 (Sigma-Aldridge, UK) benchtop vortex for one minute to achieve homogenous mixing of the two powders (see Table1). The P40 glass and the P40/yttrium oxide mixtures were processed into microspheres using a flame spheroidisation method employing an oxy-acetylene thermal spray gun (MK74, Metallisation Ltd, UK). Processed microspheres were washed with deionised water and left to dry in a 50°C oven overnight. The microspheres were then sieved into a size range of $45\text{--}125\text{ }\mu\text{m}$ using Laboratory Test Sieves (Endecotts, UK).

Table 1: The P40:Yttrium oxide ratio and the corresponding sample codes

Sample code	Ratio of P40 Glass to Yttrium Oxide
P40	100:0
10Y	90:10
20Y	80:20
30Y	70:30
40Y	60:40
50Y	50:50

Scanning electron microscopy (SEM)

Morphological analysis of the microspheres was conducted utilizing a JSM-6490LV (JEOL, USA). Selected microsphere samples were mounted on carbon tabs affixed to aluminum stubs and sputter-coated with approximately 15 nm of platinum in an argon atmosphere.

To investigate the internal structures, microspheres were embedded in cold-set epoxy resin. The resin blocks were then polished with SiC paper and a polishing cloth embedded with diamond paste down to a 1 μm finish, using industrial methylated spirit (IMS) (Sigma Aldrich, UK) as the lubricant. After polishing, the resin block was placed in an ultrasonic bath with IMS for 5 minutes and allowed to dry. Finally, the samples were sputter-coated with 15 nm of carbon using a Quorum Q150V (Quorum, UK) for EDX analysis.

Energy dispersive X-ray spectroscopy (EDX)

Compositional analysis was conducted on both microspheres mounted on carbon tabs fixed to aluminum stubs and those embedded in resin. The samples were coated with a layer of carbon using a Q150T Turbo-Pumped Sputter Carbon Coater (Quorum, UK). For energy-dispersive X-ray spectroscopy (EDX) and mapping, an Oxford Instruments INCA EDX system equipped with a Si-Li crystal detector was integrated with the JSM6490LV SEM, operating at an accelerating voltage of 15 kV and a working distance of 10 mm.

Powder X-ray diffraction (XRD)

To assess the amorphous or crystalline nature of the microspheres, a Bruker D8 Advanced X-ray diffractometer (Bruker-AXS, Karlsruhe, Germany) operating at room temperature with a Ni-filtered Cu-K α radiation source was used. Data were collected at 0.02° intervals across a 10-70° range over a duration of 10 minutes. The obtained data were then analyzed using DIFFRAC.EVA software (DIFFRAC-plus suite, Bruker-AXS), which facilitated phase identification by referencing the International Centre for Diffraction Data (ICDD) 2021 database.

Ion release studies

The ion release profiles of the microspheres were assessed, according to the method previously described in [9], by immersing 400 mg of the microspheres in 40 mL of ultrapure MilliQ water at 37°C. At each time interval (3, 7, 14, 21, and 28 days), the dissolution medium was filtered and replaced. The concentrations of sodium, phosphorus, calcium, magnesium, and yttrium ions were quantified using inductively coupled plasma mass spectrometry (ICP-MS, ThermoFisher iCAP-Q model). Additionally, the pH of the solutions was recorded at each time point with a pH electrode InLab Pure Pro-ISM (Mettler Toledo, UK).

Microsphere sterilisation and preparation of conditioned media

As described by Milborne et al., sterilization of the microspheres was achieved through two successive 10-minute washes with 100% ethanol. Following this, the microspheres were allowed to dry completely overnight at room temperature

within a sterile Class 2 microbiological safety cabinet to ensure aseptic conditions and reduce the risk of microbial contamination.

For preparing the conditioned medium with microsphere ion extracts for MG63 cells, 100 mg/mL of sterile microspheres were incubated in standard cell culture medium (DMEM supplemented with 10% fetal calf serum, 1% penicillin-streptomycin, 1% L-Glutamine, 1% nonessential amino acids, and 1.5% ascorbic acid; ThermoFisher, UK) at 37°C with 5% CO₂. The conditioned medium, containing the ion extracts, was collected and replaced with fresh medium of equal volume every 48 hours. Prior to administration to the cells, the solutions were filtered through 0.22 μm syringe filters to eliminate any debris or precipitate [9].

In vitro indirect cell culture studies

For the indirect culture method using microsphere-conditioned media, the human osteoblast-derived cell line MG63 (obtained from European collection of cell cultures - ECACC) were seeded at a density of 10,000 cells/cm² in 300 μL of standard cell culture medium in 48-well plates. After 48 hours, cells were washed with PBS and 300 μL of the corresponding conditioned media was added. Control groups included cells cultured with either unconditioned standard medium (+ve), or standard cell culture medium supplemented 5% DMSO (-ve). Media was refreshed every 48 hours. The experiment was conducted with two independent biological replicates, each including three experimental replicates per condition [9].

In vitro direct cell culture studies

Direct seeding of cells onto the microspheres was performed according to the method previously described in [9]. Low-adherent 48-well plates (Sigma Aldrich, UK) were coated with 1% (w/v) solution of poly(2-hydroxyethyl methacrylate) (poly-HEMA, Sigma-Aldrich, UK). This was accomplished by dissolving powdered poly-HEMA in pre-heated 65°C absolute ethanol, applying the solution to the well plates and incubating them overnight at 37 °C to allow for ethanol evaporation. The plates were washed three times with PBS. 10 mg sterilised microspheres from each formulation were added to the wells and MG63 cells were seeded at a density of 10,000 cells/cm². Each well received 300 μL of standard cell culture medium. Cells were cultured for 7 days at 37 °C and 5% CO₂, with media changes occurring every 48 hours.

Cell metabolic activity

The metabolic activity of MG63 cells was assessed on days 2 and 7 using the Alamar Blue assay. To each well, 300 μL of Alamar Blue solution (prepared as a 1:9 mixture of Alamar Blue and Hank's Balanced Salt Solution) was added and incubated for 90 minutes at 37°C with 5% CO₂, followed by an additional 10 minutes of shaking at 150 rpm. From each condition, three 100 μL aliquots were transferred to a 96-well plate. Fluorescence measurements were conducted using a FLx800 fluorescence microplate reader (BioTek Instruments Inc.) with excitation at 530 nm and emission at 590 nm [45].

Alkaline phosphatase (ALP) activity

On day 7, the cells were washed three times with warm (37°C) PBS and then immersed in 1 mL of deionized water. The samples underwent three freeze-thaw cycles to lyse the cells and release their nuclear content. ALP activity in MG63 cells was quantified using the Granutest 25 ALP assay (Randox, UK). Three 50 μ L aliquots of the cell lysate were placed into a 96-well plate, each followed by 50 μ L of ALP substrate (p-nitrophenyl phosphate at 10 mM in a diethanolamine buffer at 1 mM, pH 9.8, with 0.5 mM MgCl₂). The plates were gently shaken for 5 minutes, and absorbance was measured at 405 nm with an FLx800 microplate colorimeter (BioTek Instruments) every 5 minutes for 45 minutes, until the readings stabilized. This procedure was applied to cells grown under both indirect and direct culture conditions.

DNA content assay

Cell lysates used for ALP activity measurement were thoroughly mixed for 30-60 seconds using a vortex mixer, and 100 μ L of each sample was transferred into a 96-well plate. Hoechst 33258 stain was prepared by dissolving 1 mg of BisBenzimide in 1 mL of double-distilled water and then diluting the solution to a 1:50 ratio in TNE buffer. DNA standards were created using calf thymus DNA (Sigma, UK) and TNE buffer (10 mM Tris, 2 M NaCl, and 1 mM EDTA in deionized water, adjusted to pH 7.4) to establish a standard curve for DNA concentration. To each well, 100 μ L of Hoechst 33258 stain was added and mixed on a plate shaker for 5 minutes at 150 rpm. The fluorescence was measured using an FLx800 plate reader (BioTek Instruments) with an excitation wavelength of 360 nm and an emission wavelength of 460 nm.

Statistical analysis

Two independent experiments were performed, and results are presented as mean \pm standard error of mean unless specified otherwise. Statistical analysis was performed using Prism software package (version 9.2.0, GraphPad Software, San Diego, CA, www.graphpad.com). Two-way analysis of variance was performed, followed by a Tukey's multiple comparison test. The mean difference was deemed statistically significant at a threshold of 0.05 with a 95% confidence interval.

Cell imaging

For imaging of cell attachment to microspheres, at day 7 the MG63s were washed three times with warm (37°C) PBS and fixed with 4% paraformaldehyde for 10 minutes. Fixative was then removed, and the sample washed twice deionised water. For Environmental Scanning Electron Microscopy (ESEM), after fixation, microspheres and cells were carefully isolated using a glass pipette and mounted onto the stage of the FEI Quanta 650 ESEM microscope for analysis.

Results

Morphological Analysis

SEM analysis revealed that after processing the glass particles via flame spheroidisation and sieving within a 45 – 125 μ m size range, a high yield of spherical microspheres were produced. As seen in Figure 1, a lack of aggregation and a narrow size distribution was achieved using this process for each of the yttrium oxide to glass ratio samples prepared prior to spheroidisation.

Compositional Analysis

EDX analysis was performed to confirm the chemical composition of the microspheres manufactured at each yttrium oxide to glass ratio explored. As the amount of yttrium oxide mixed with the glass prior to processing increased, a subsequent significant increase in yttrium content within the microspheres was observed. The yttrium oxide content increased from ~0.8 mol %, 7.5 mol %, 15.0 mol %, 25.1 mol % and 39.1 mol % for the 10Y, 20Y, 30Y, 40Y and 50Y microspheres respectively. However, a proportional decrease in all the other glass elements was also observed (see Figure 2A). Phosphate content decreased from ~36 mol % in P40 and 10Y microspheres to 23.6 mol % within 50Y microspheres. Calcium oxide content decreased from 16.8 mol % in P40 microspheres to 19.6 mol %, 16.6 mol %, 15.5 mol %, 14.0 mol % and 11.7 mol % for the 10Y, 20Y, 30Y, 40Y and 50Y microspheres respectively. Similarly, magnesium oxide content decreased incrementally when moving through the series from 10Y to 50Y. Magnesium oxide content in 50Y microspheres of 19.3 mol % was approximately two thirds of the content of the magnesium oxide content in comparison to P40 microspheres (27.3 mol %).

To explore distribution of the elements within the microspheres produced, EDX mapping (of representative resin embedded microspheres which were then subsequently polished to reveal the inner structure) of P40, 30Y and 50Y microspheres was performed. For P40 microspheres, all the glass forming elements (O, N, Mg, P, Ca) were distributed evenly throughout the microspheres. The yttrium-containing microspheres had the same elements detected as well as yttrium being homogeneously distributed throughout the whole body of the microspheres (see Figure 2B).

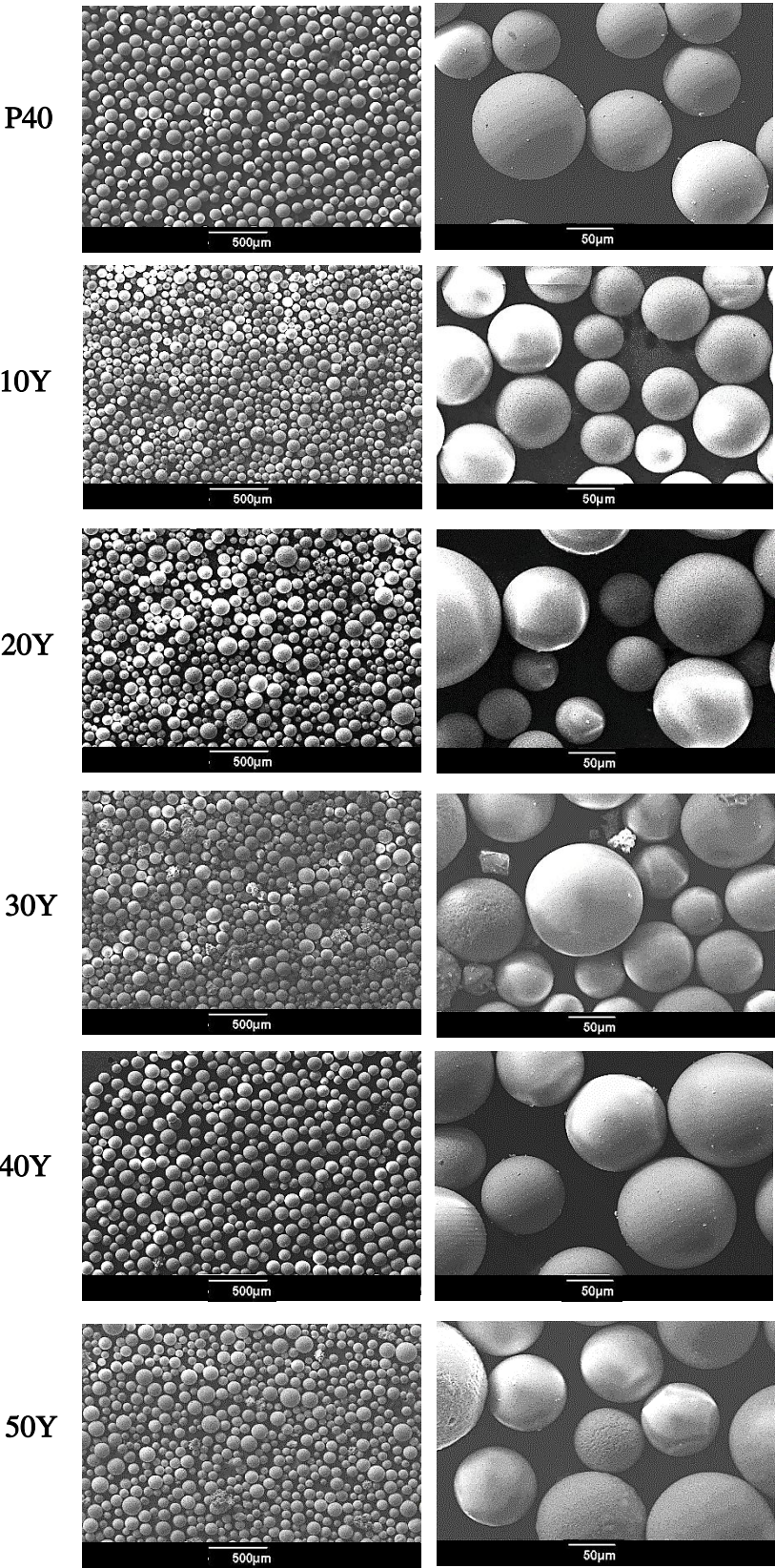


Figure 1: SEM images depicting the morphology of the yttrium-containing microspheres produced.

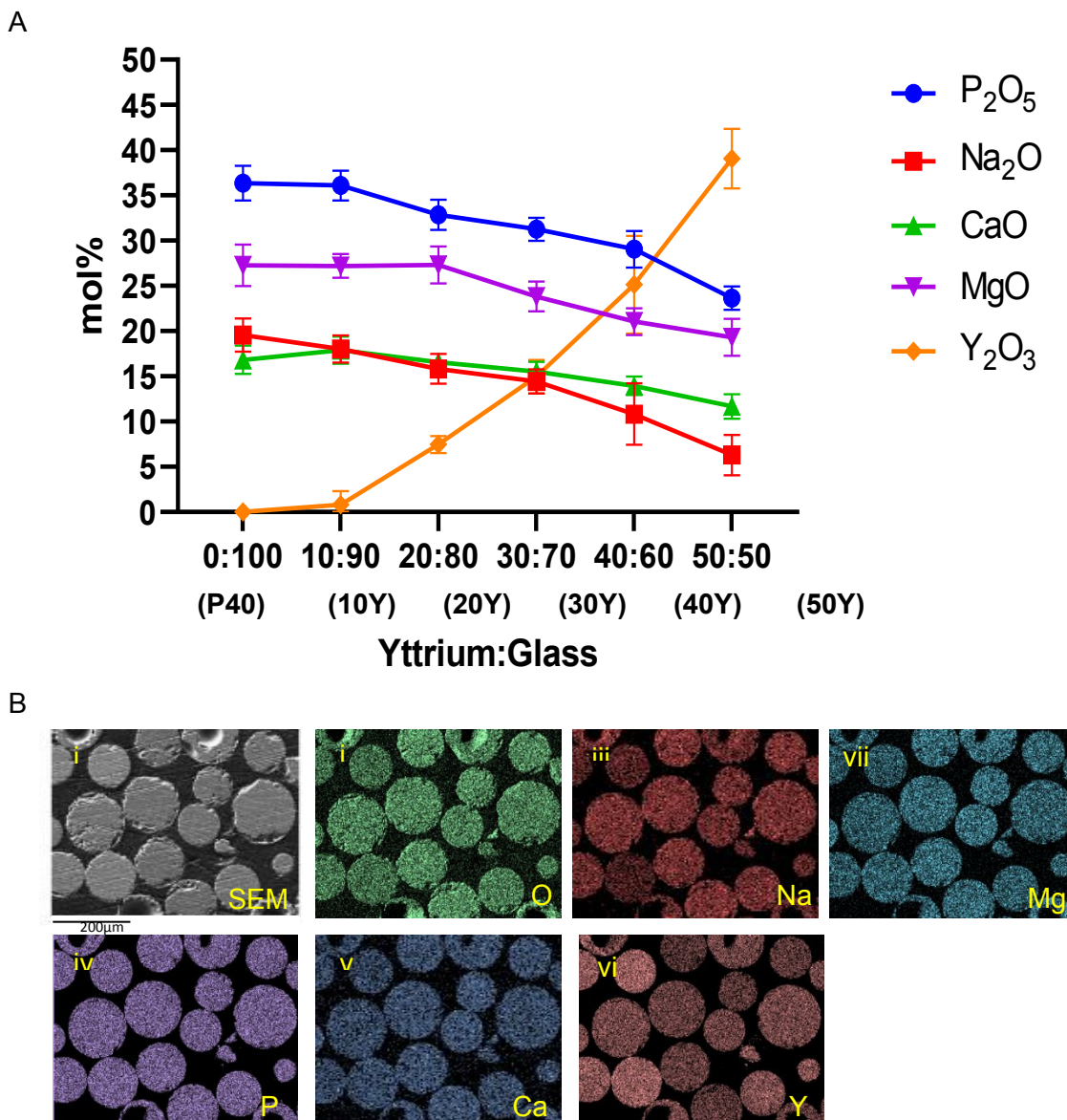
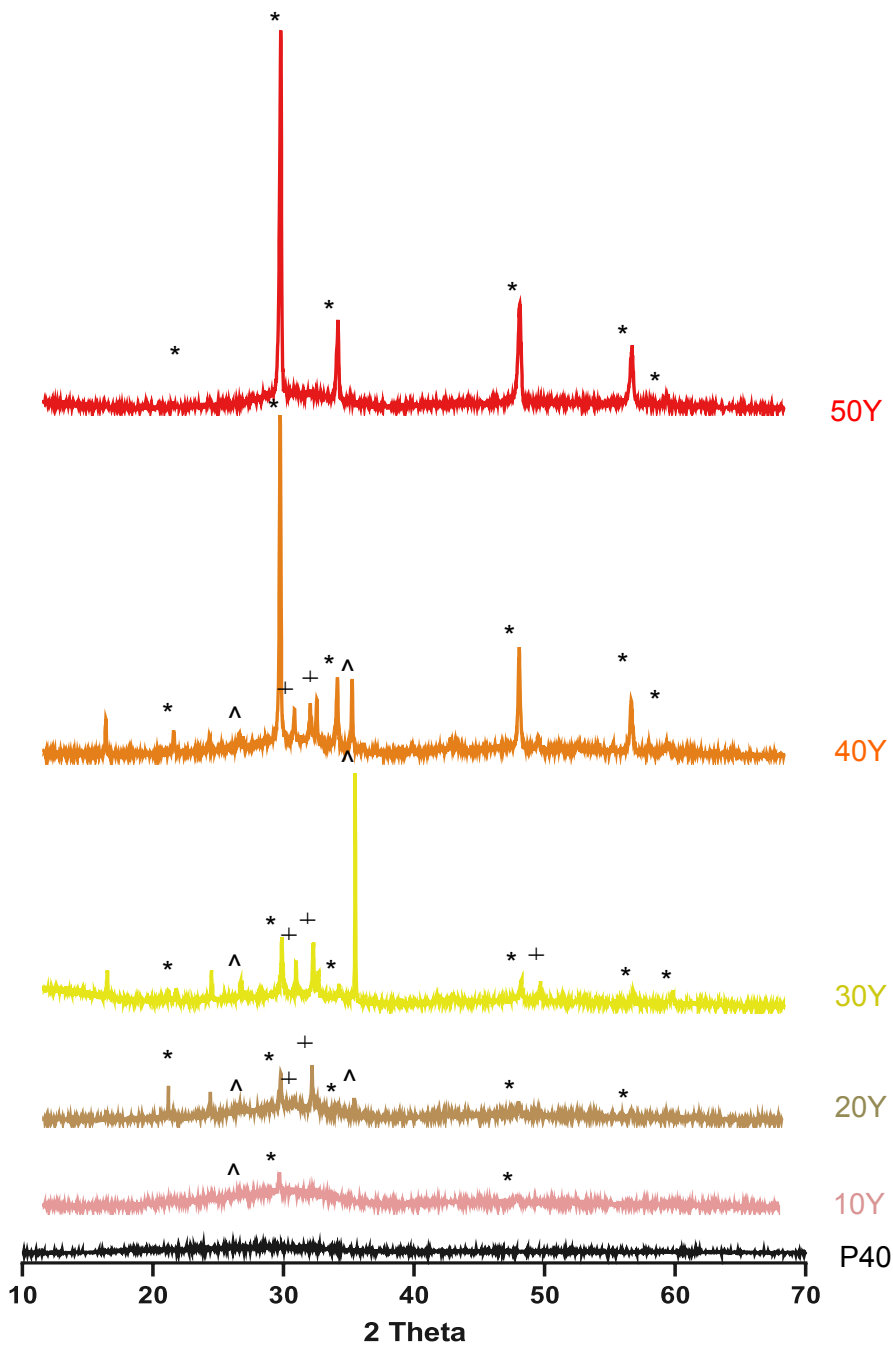


Figure 2: (A) Elemental composition determined EDX of the yttrium-containing microspheres produced via flame spheroidisation. Results are presented as mean \pm standard error of mean ($n=10$) (B) EDX mapping of resin embedded 30Y microspheres showing the homogenous distribution of all the elements throughout the microspheres produced (i) SEM image of resin embed and polished samples (ii) Oxygen (iii) Sodium (iv) Magnesium (v) Phosphorous (vi) Calcium (vii) Yttrium content observed.

XRD Analysis

Figure 3 shows the XRD profiles for the solid microspheres made from the P40 parent glass and at each yttrium:glass ratio. A single broad halo peak at 2θ values of ~ 30 – 32° was observed for the P40 solid microspheres and the absence of any detectable crystalline peaks confirmed the amorphous nature of the

glass microspheres produced. The profiles for the yttrium-containing microspheres post processing, revealed the presence of sharp crystalline peaks. For the 10Y sample, peaks at $\sim 29^\circ$ and 49° were observed, which were matched to cubic Y₂O₃ according to powder diffraction file 01-079-1257 (ICDD database). An additional peak at $\sim 26^\circ$ was also seen which corresponded to Y(PO₄) (ICDD 01-084-0335). For the 20Y microspheres, sharp peaks at $\sim 29^\circ$, 34° , 49° and 58° were observed, which were matched to cubic Y₂O₃ (01-079-1257 ICDD) as well as peaks at $\sim 26^\circ$ and 35° which corresponded to Y(PO₄) (ICDD 01-084-0335). Additional peaks were also seen at $\sim 30^\circ$ and 32° which were matched to hexagonal Y₂O₃ according to powder diffraction file 01-076-7397 (ICDD database). Both 30Y and 40Y microspheres showed the same peaks corresponding to cubic Y₂O₃ (01-079-1257 ICDD), Y(PO₄) (ICDD 01-084-0335) and also hexagonal Y₂O₃ (01-076-7397 ICDD). The 50Y microspheres profile, only showed peaks at $\sim 29^\circ$, 34° , 49° , 58° and 61° 2θ values which corresponded to cubic Y₂O₃ (according to the file 01-079-1257 ICDD database).



From here on only the 30Y and 50Y microspheres were chosen for further characterisation and study. The 30Y was selected due to its yttrium content ($\sim 15.0 \text{ mol}\% \pm 1.8$) being comparable to that of Therasphere and containing a P_2O_5 content of $\sim 30 \text{ mol}\%$. Whilst, 50Y microspheres were selected as these had the highest yttrium content ($39.1 \text{ mol}\% \pm 3.3$).

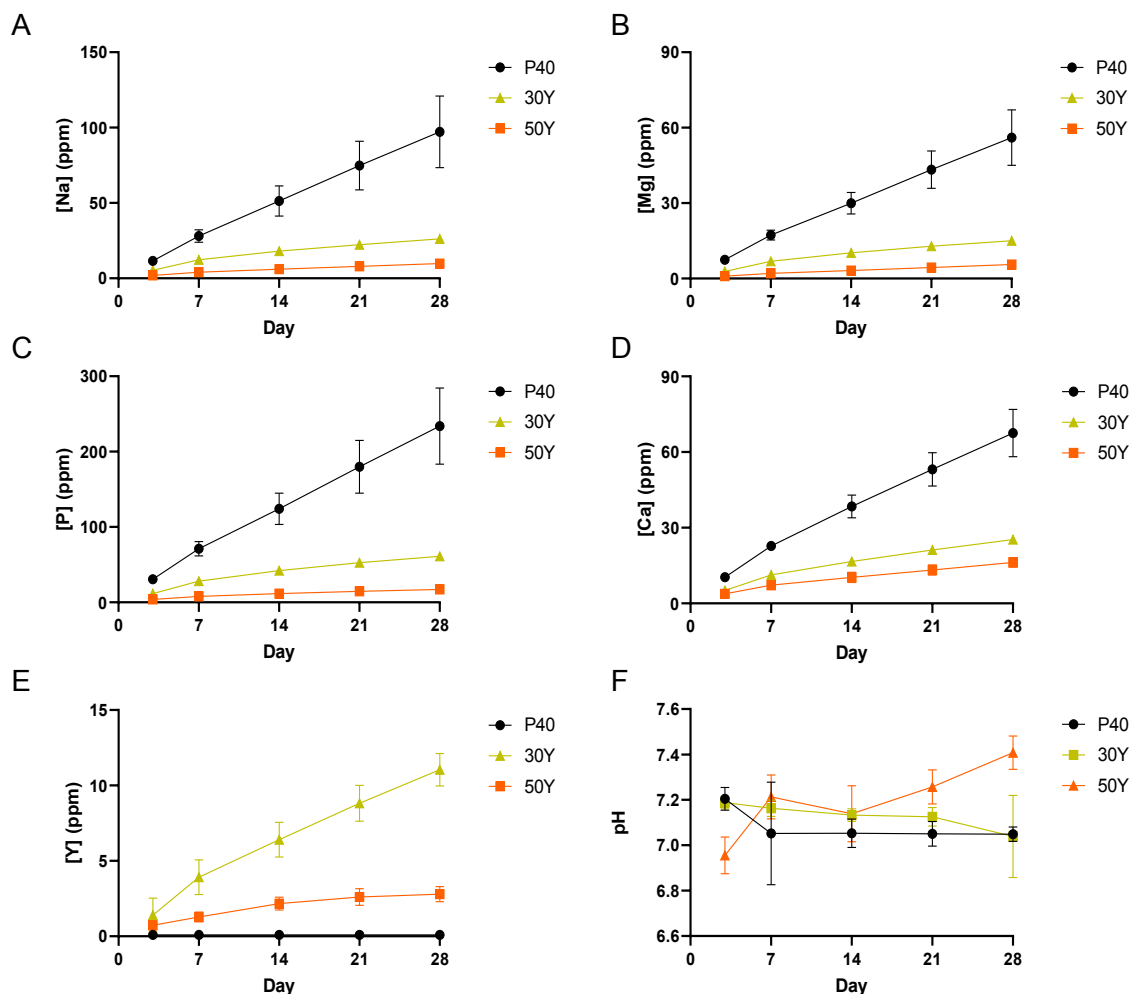
Figure 3: XRD spectra of P40 SMS (black), 10Y, 20Y 30Y (gold), 40Y and 50Y (orange) solid microspheres. The crystalline peaks matched for cubic Y_2O_3 (*), hexagonal Y_2O_3 (+) and $Y(PO_4)$ (^).

Ion release studies

Ion release studies were performed to assess the durability of the yttrium-containing microspheres compared to P40 microspheres and the effect of yttrium addition on ion release kinetics.

Figure 4 shows the cumulative ion release profiles for P40, 30Y and 50Y solid microspheres calculated from measurements obtained via ICP analysis over 28 days. The ions released from each formulation exhibited a linear relationship with time and were released consistently. The P40 solid microspheres degraded much faster than the 30Y and 50Y microspheres, revealing ion release rates which were statistically significant and higher in comparison to the yttrium-containing microspheres (i.e. Na and P: $p < 0.0001$; Mg and Ca: vs 30Y $p < 0.01$, vs 50Y $p < 0.001$). As the yttrium content in the microspheres increased, a decrease in the ion release rates was also observed.

Figure 4F illustrates the pH changes in Milli-Q water during the 28-day immersion of the microspheres. For the solution with P40 solid microspheres, the pH dropped from ~ 7.2 on day 3 to ~ 7.0 by day 7, and then remained stable for the remainder of the study. 30Y solution had a comparable value to the P40 sample at both day 3 and day 28 albeit with a slight decrease in pH which occurred more gradually. A pH of ~ 6.9 for 50Y was observed at day 3 which then increased to ~ 7.4 by the end of the 28-day period.



The P40 microspheres released Na^+ (~ 3.5 ppm/day), Mg^{2+} (2.0 ppm/day), and P (8.4 ppm/day) at an approximate rate around 3.5 times greater than that of the 30Y microspheres and around 10 times higher rate compared to 50Y microspheres. P was the only ion that was released at a statistically significant higher release rate (2.2 ppm/day) from 30Y microspheres in comparison to 50Y microspheres (0.6 ppm/day) ($p < 0.01$). The yttrium containing microspheres released only very small amounts of yttrium ions in comparison to all the other elements. The 30Y microspheres revealed the highest release rate of Y^{3+} ions (at ~ 0.4 ppm/day), whereas the 50Y microspheres, which contained a greater amount of yttrium, revealed an approximate release rate of 0.1 ppm/day.

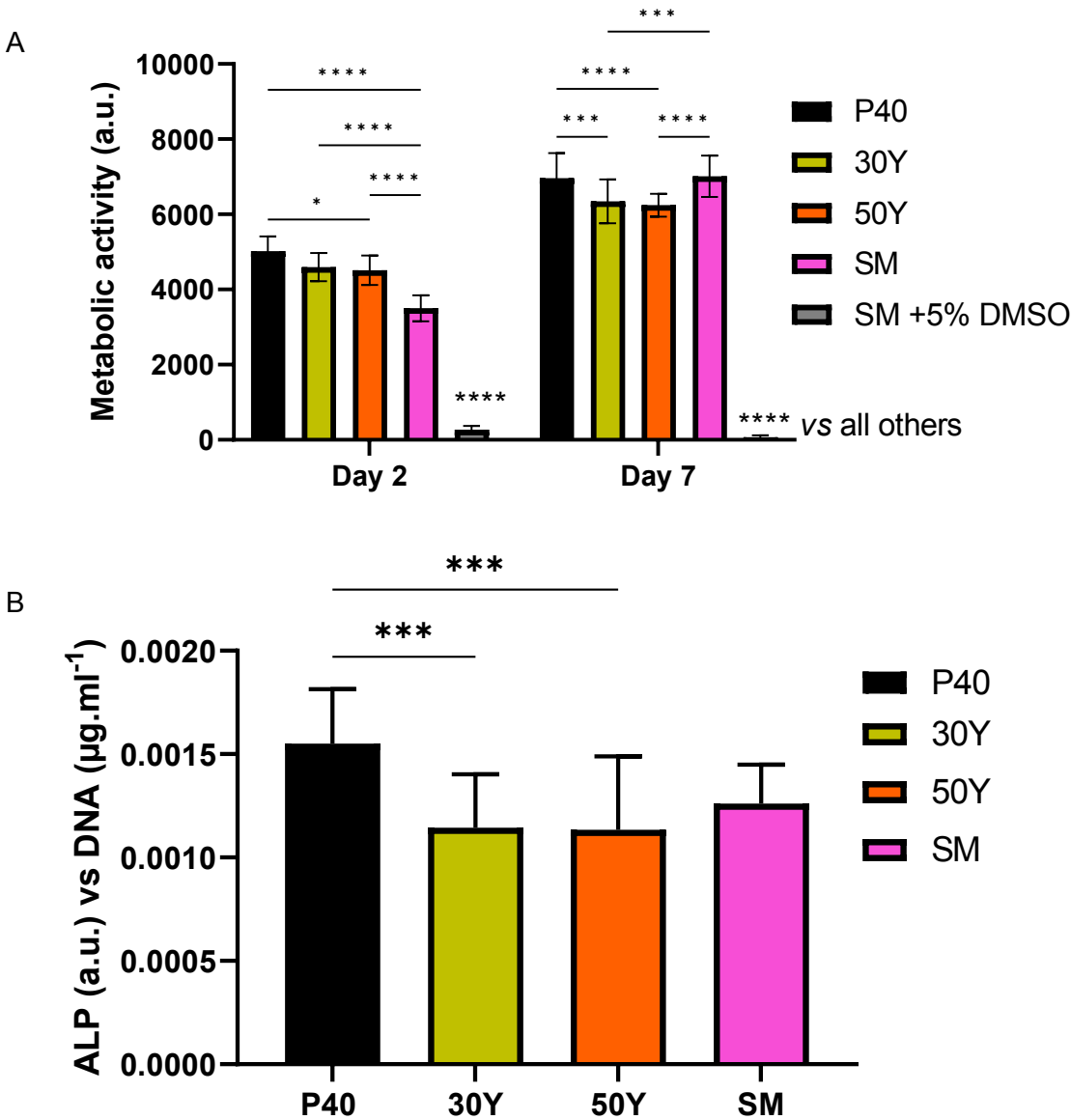
Figure 4: Cumulative ion release profile of (A) [Na], (B) [Mg], (C) [P], (D) [Ca] and (E) [Y] measured via ICP-MS of solid P40, 30Y and 50Y microspheres immersed in milli-Q water over a 28 day period. (F) pH of milli-Q water during 28 days of P40, 30Y and 50Y solid microspheres immersion within the solution. (Standard deviation error bars are also included in the data above, three independent repeats were performed for studies at each time for each microsphere composition).

Indirect in vitro cell culture studies

To assess the cytocompatibility of the produced microspheres, an indirect cell culture approach was used. This method

involved treating osteoblast-like MG63 cells with media conditioned by the microspheres to analyze their biological responses

statistically significant increased metabolic response compared to the yttrium- formulations ($p < 0.001$), however no statistically significant differences were detected between P40



to the dissolution products released over time. Standard medium (SM) and SM with 5% DMSO served as positive and negative controls, respectively. Analysis of metabolic activity via the Alamar Blue assay showed a significant increase in cell response when both 30Y and 50Y microspheres conditioned media was added between day 2 to day 7 (D2 vs D7: $p < 0.0001$). This increase in metabolic activity was also seen for cells treated with SM but cells where SM + 5% DMSO was applied, revealed no apparent increase in metabolic activity from day 2 to day 7 (D2 vs D7: $p < 0.0001$). At day 2, cells treated with P40, 30Y and 50Y conditioned media had a significantly greater metabolic response compared to those treated with SM and SM + 5% DMSO ($p < 0.0001$). No statistically significant difference was observed between cells treated with 30Y and 50Y conditioned media ($p > 0.05$). There was also no statistically significant difference between the cells treated with 30Y and 50Y conditioned media at day 7 ($p > 0.05$). At day 7, cells treated with P40 and SM media revealed a

and SM ($p > 0.05$) (see Figure 5A).

Figure 5: (A) Evaluation of cell metabolic activity in indirect culture of P40, 30Y and 50Y solid microspheres at day 2 and day 7. **** $p < 0.0001$, *** $p < 0.001$, * $p < 0.05$. (B) Evaluation of ALP activity in indirect culture of P40, 30Y and 50Y solid microspheres at day 7. *** $p < 0.001$. Results are presented as mean \pm standard error of mean. Two independent experiments were performed, each with $n=3$ replicate wells.

Alkaline phosphatase (ALP) activity was also measured as an early marker of osteogenic differentiation in MG63 cells after 7 days of indirect culture from P40, 30Y and 50Y microsphere formulations and SM. The ALP activity was normalised to the DNA content of the cells under investigation. At day 7, there was no statistically significant difference in ALP activity between cells grown in SM and both 30Y and 50Y conditioned

media ($p > 0.05$). Cells grown in P40 media had statistically significantly higher ALP activity compared to cells grown in the two yttrium-containing microsphere media (vs 30Y and 50Y: $p < 0.001$) (see Figure 5B).

Direct in vitro cell culture studies

MG63 cells were also directly seeded onto P40, 30Y and 50Y solid microspheres to assess the effect of direct physical contact on cellular responses and the microspheres' ability to provide a suitable surface to facilitate cell growth and proliferation. Analysis of metabolic activity at day 2, revealed that there was no statistically significant difference in metabolic activity between cells grown on P40 microspheres and the two yttrium-containing microsphere formulations ($p > 0.05$). Cells cultured on 30Y microspheres revealed higher metabolic activity at day 2 compared to those grown on 50Y ($p < 0.05$). Cells grown on any of the three microsphere formulations displayed statistically significant lower metabolic activity compared to TCP control ($p < 0.0001$) (see Figure 6A).

Also, a statistically significant higher metabolic activity was seen in cells cultured on each of the three microsphere formulations and TCP at day 7 in comparison to day 2 ($p < 0.0001$). At day 7, no statistically significant difference in metabolic activity between the cells cultured on 30Y and 50Y microspheres ($p > 0.05$) was observed. However, metabolic activity was statistically significant lower than those cultured on P40 microspheres (vs 30Y: $p < 0.01$; vs 50Y: $p < 0.001$) (see Figure 6A).

After 7 days the ALP activity of MG63s grown directly on the microspheres and TCP was determined and normalised to the DNA concentration. Statistically significant higher ALP activity was recorded for cells grown on P40, 30Y and 50Y microspheres in comparison to those grown on the TCP control ($p < 0.0001$). There was no statistically significant difference in ALP activity detected between cells grown on P40 and the two yttrium-containing microsphere formulations ($p > 0.05$) (see Figure 6B).

MG63 cells directly cultured onto the microspheres were visualised using ESEM at day 7. Cells were seen adhered onto the P40, 30Y and 50Y microsphere surfaces and appeared to be displaying lamellipodia and filopodia projections, which bridged adjacent neighbouring microspheres and were spread over the microsphere surfaces (see Figure 6C).

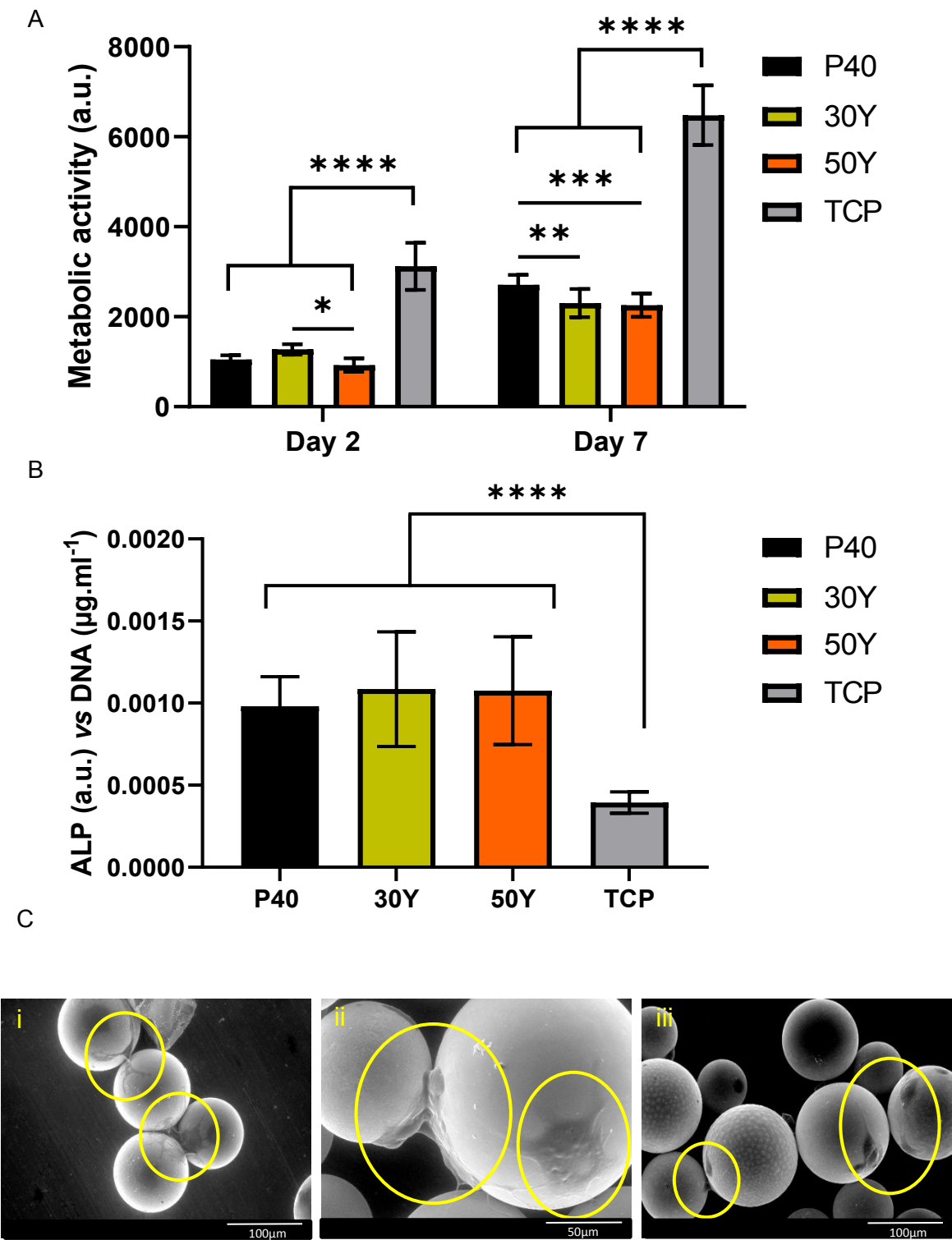


Figure 6: (A) Evaluation of cell metabolic activity in direct culture of P40, 30Y and 50Y solid microspheres at day 2 and day 7. **** $p < 0.0001$, *** $p < 0.001$, ** $p < 0.01$, * $p < 0.05$. Results are presented as mean \pm standard error of mean. Two independent experiments were performed, each with $n=3$ replicate wells. (B) Evaluation of ALP activity in direct culture of

P40, 30Y and 50Y solid microspheres at day 7. *** $p < 0.001$. Results are presented as mean \pm standard error of mean. Two independent experiments were performed, each with $n=3$ replicate wells. (C) SEM images of (i) P40 (ii) 30Y and (iii) 50Y solid microspheres after 7 days direct culture with MG63 cells.

The yellow circles highlight areas where cells have attached and formed colonies on the surface of the microspheres.

Discussion

In this work a novel processing method was developed to significantly increase the level of yttrium content that could be incorporated into phosphate-based glass [23]. A study by Arafat *et al.* investigating the crystallisation behaviour of glasses within the system $45\text{P}_2\text{O}_5 - (30 - x)\text{Na}_2\text{O} - 25\text{CaO} - x\text{Y}_2\text{O}_3$ — (where $x = 0$ to 10) found that the addition of Y_2O_3 was limited to ~ 5 mol%, when attempting to prepare the formulations via conventional glass melt processes, as further addition resulted in crystallisation of the glass [20]. This demonstrated the difficulties often encountered when trying to incorporate high quantities of Y_2O_3 within a phosphate-based glass. The current methodology developed allowed for the yttrium content to be varied by simply altering the Y_2O_3 to glass particle ratios prior to the spheroidisation process. This resulted in the production of uniform solid microspheres containing varying yttrium levels (ranging from ~ 1 mol% to 39 mol %). This method was capable of producing microspheres that had equivalent and enhanced yttrium content, in comparison to clinically available aluminosilicate glass microspheres used for internal radiotherapy applications (Therasphere). The 30Y microspheres were chosen for further characterisation and study due to their yttrium content ($15 \text{ mol}\% \pm 1.8$) being comparable to that of Therasphere, whilst also containing a P_2O_5 content of ~ 30 mol%. The 50Y microspheres were studied further as these had the highest yttrium content ($39 \text{ mol}\% \pm 3.3$) and it was postulated that they may retain some of the beneficial features from their parent P40 glass, such as release of therapeutic ions (such as Ca, Mg and Na). The authors believe that the yttrium oxide content achieved within the 50Y microspheres composition is the highest achieved within a phosphate-glass matrix to produce uniform microspheres.

In addition to elevated yttrium content, microspheres offer enhanced delivery characteristics compared to irregularly shaped particles and can be effectively administered through minimally invasive surgical injection techniques.[24]. This is important for internal radiotherapy applications, where the ability to administer them easily and accurately is vital in order to maximise their therapeutic efficacy [25].

EDX analysis confirmed that the addition of Y_2O_3 resulted in the formation of microspheres that had reduced content of all elements present in the parent P40 glass formulation after processing. With increasing Y_2O_3 addition proportional decreases in these elements were observed (Figure 2A). EDX mapping of resin embedded 30Y and 50Y microspheres was performed to establish whether any of the elements were concentrated at regions within the microspheres. The mapping showed that all the elements were homogeneously distributed throughout the whole of the yttrium-containing microspheres and did not appear to be concentrated at the surface (see Figure 2B). Tesfay *et al.* produced Y-doped bioactive glass spherical powders based on 58S (60 mol% SiO_2 , 35 mol% CaO , and 5 mol% P_2O_5) using a spray pyrolysis method. They also achieved local Y distribution dispersed homogeneously throughout their particles. However, the Y content was only 7 to 11 mol % and particles were less than $1 \mu\text{m}$ in size [26]. Ghahramani *et al.* obtained yttrium aluminium silicate microspheres, around 20 –

$50 \mu\text{m}$ in size, using a sol-gel method via an aqueous solution of $\text{Y}(\text{NO}_3)_3$ and $\text{Al}(\text{NO}_3)_3$ being added to tetraethyl orthosilicate (TEOS) and pumped into stirred silicone oil. In their study, SEM and EDX analysis revealed that the microspheres consisted of two parts: the crust and the core. Y and Al were shown to be distributed in the core, whereas Si was distributed in the crust, which appeared at the periphery the microspheres [27]. Sol-gel methods are time-consuming and labour intensive due to their multi-step nature, with a lengthy methodology required to remove residual contaminants. In the present study, a novel single-stage flame spheroidisation method was used to rapidly produce high yttrium-containing phosphate-based microspheres with homogenous elemental distribution. Homogenous size distribution and desired size range can be achieved using Laboratory Test Sieves into specific and desired size ranges.

It is proposed that a high yttrium content in the microspheres would be desirable for radiotherapy applications as it may enable more radiation to be delivered per dose of microspheres, leading to the use of fewer microspheres [28]. A higher yttrium content may also result in shorter neutron activation times and aid with logistical issues involving the time and transportation of the microspheres from the nuclear activation facility to the clinic. Nuclear decay occurs during this period and the greater the amount of radioactivity, the longer the transit time available in order for the patient to still receive an efficacious radiation dose [29]. Future research involving neutron activation studies are required to empirically validate that yttrium-containing microspheres can generate therapeutically relevant doses of irradiation. Quantification of the actual radiation dose emitted by the activated ^{90}Y within the microspheres would allow identification and design of the optimal formulation to maximise therapeutic efficacy with minimal adverse effects.

The XRD profiles for the yttrium-containing microspheres produced, revealed the presence of crystalline peaks, indicating that the microspheres produced were glass-ceramic in nature and not amorphous samples (see Figure 3). The 10Y microsphere samples had peaks that corresponded to cubic Y_2O_3 (ICDD 01-079-1257) and $\text{Y}(\text{PO}_4)$ (ICDD 01-084-0335). Peaks that corresponded to these two phases were present in 20Y, 30Y and 40Y microspheres as well as additional peaks that corresponded to the hexagonal phase of Y_2O_3 (ICDD 01-076-7397). The 50Y microspheres, which contained the highest yttrium content, only revealed peaks corresponding to the cubic phase of Y_2O_3 (ICDD 01-079-1257). Similar results were also seen in a study by Kawashita *et al.* where ceramic microspheres were formed from solely Y_2O_3 or YPO_4 powder using a high-frequency induction thermal plasma melting technique at flame temperatures estimated between $12,000$ and $13,000^\circ\text{C}$ [30]. Only peaks that corresponded to cubic Y_2O_3 were detected in the Y_2O_3 microspheres, whereas weak diffraction peaks corresponding to both cubic and monoclinic Y_2O_3 were identified in addition to YPO_4 peaks in the YPO_4 derived microspheres. For the YPO_4 microspheres, it was found that the intensity of the YPO_4 peaks decreased, whilst the Y_2O_3 peaks increased with increasing plasma flame power. This was attributed to the loss of P_2O_5 due to volatilisation. Similarly, the decreased P_2O_5 content within 50Y microspheres compared to 40Y, 30Y and 20Y may have prevented the formation of a YPO_4 phase.

The addition of yttrium to phosphate glass microspheres not only facilitated their potential use as a vector for radiotherapy delivery but also improved significantly the durability of phosphate glasses [31]. Other transition oxides such as TiO_2 , Al_2O_3 and Fe_2O_3 have been incorporated into phosphate glasses and have been shown to improve some of the physical properties, such as their rapid degradation within aqueous media that can limit their clinical applications [32–34]. The addition of certain transition oxides have been shown to decrease degradation rates within phosphate-based glasses by up to 3 to 4 orders of magnitude [35]. Classical molecular dynamics simulations conducted on the structure of yttrium doped phosphate-based glasses showed that yttrium oxide up to 6 mol% acted as a network modifier and resulted in depolymerisation of the phosphate network within quaternary phosphate glasses [36].

A study by Arafat *et al.* investigated the role of yttrium in phosphate-based glasses in the system $45(\text{P}_2\text{O}_5) - 25(\text{CaO}) - (30 - x)(\text{Na}_2\text{O}) - x(\text{Y}_2\text{O}_3)$ mol% ($0 \leq x \leq 5$) prepared via melt quenching [20]. Depolymerisation of the glass network was seen with increasing yttrium oxide addition. ^{31}P NMR analysis showed an increase of Q^1 species, from 23 to 42%, which was accompanied by a corresponding decrease of Q^2 species from 77 to 58% as Y_2O_3 addition increased from 0 to 5%. The increasing Y_2O_3 content also resulted in a decrease in the phosphate chain length, which was further evidence of depolymerisation and the dissociation of metaphosphate chains. As a network modifier, Y^{3+} can occupy the interstitial space between PO_4 tetrahedra and bond with phosphate glass terminal oxygen's causing a decrease in bridging oxygen's (BO) and an increase in non-bridging oxygen's (NBO). Previous studies have concluded that yttrium perturbs the glass network strongly, by stabilising the formation of negatively charged species such as non-bridging oxygen atoms [37]. Due to it being a high field strength trivalent cation, yttrium forms strong cross-linking Y-O-P bonds between phosphate chains. Yttrium's field strength ($\sim 0.60 \text{ e } \text{\AA}^{-2}$) is significantly higher than that of magnesium ($\sim 0.46 \text{ e } \text{\AA}^{-2}$), calcium ($\sim 0.33 \text{ e } \text{\AA}^{-2}$) and sodium ($\sim 0.19 \text{ e } \text{\AA}^{-2}$) and this leads to the formation of stronger bonds within the phosphate glass network and explains why an increase in chemical durability was seen with increasing Y_2O_3 content [21, 38].

Previous studies showed that the increase in cross-linking of the phosphate network with the addition of Y_2O_3 causes a decrease in the degradation of the glasses, since Y-O-P bonds are more resistant to hydration attack than P-O-P bonds [39]. Classical molecular dynamics simulations showed that when yttrium was incorporated into a ternary phosphate glass series it bonded to a greater number of phosphate chains (4.2 – 4.3) in comparison to both calcium (3.8) and sodium (3.1–3.2) [36], leading to strengthening of the glass against dissolution. Decreased degradation results in a lower ion release profiles which would be beneficial when developing glasses for radiotherapy applications [40]. The glass needs to be durable whilst the yttrium is radioactive to avoid leaching of the radionuclide and irradiating the patient away from the target site. In the aforementioned studies on yttrium incorporation within phosphate-based glasses, the Y_2O_3 content remained relatively low, less than 6%, due to crystallisation of the glass at higher Y_2O_3 content.

However, the yttrium content in 30Y and 50Y microspheres of ~ 15 and 39 mol % was significantly higher than anything obtained and studied previously in phosphate glasses. Extensive depolymerisation of the network occurred and crystalline phases were present throughout the bulk of the microspheres. The presence of crystalline phases in the yttrium-containing glass-ceramic microspheres likely plays a significant role in the observed slower ion release rates compared to the fully amorphous P40 microspheres. Compared to the more disordered structure of an amorphous glass, the organised crystal lattice presents a greater obstacle for ion movement within the material and the crystalline phases, such as YPO_4 , can act as diffusion barriers for yttrium ions. This hinders the release of ions from the yttrium-containing glass-ceramic microspheres into the surrounding solution.

Ion release studies demonstrated that increased yttrium content resulted in a reduction in the release of all ions present in the microspheres. P40 microspheres released phosphorus, calcium, magnesium and sodium at significantly greater rates in comparison to those observed from 30Y microspheres. Furthermore, the release rate of all of these elements was significantly greater from 30Y microspheres in comparison to those observed from 50Y microspheres. Yttrium was released at the lowest rate from 30Y and 50Y microspheres in comparison to all the other elements. Despite 50Y microspheres containing more than twice the yttrium content in 30Y microspheres, the 30Y microspheres released approximately 4 times the amount of yttrium ions over 28-day immersion (Figure 4). However, at an approximate release rate of 0.4 ppm/day and 0.1 ppm/day for 30Y and 50Y microspheres respectively, the overall content released remained extremely low. Depending on the specific crystalline phases formed, the yttrium might be incorporated into more chemically stable environments compared to the amorphous glass network. This can reduce the tendency of yttrium ions to leach out during dissolution. The high durability of yttrium-containing microspheres (30Y and 50Y) is beneficial to prevent yttrium leaching. This durability also ensures localised and sustained radiotherapeutic effects, minimising irradiation of non-target tissues and supporting long-term treatment efficacy.

It is expected in physiological or buffered media, such as simulated body fluid (SBF), that an even slower ion release profiles would be observed. The complex interplay of pH, ionic strength, ion interactions and biomolecules within these solutions collectively can affect the dissolution kinetics. Surface layers may form on the glass or glass-ceramic surface leading to reduced ion release rates [41]. The yttrium-containing microspheres must have high chemical durability and resistance to degradation within bodily fluids to be used for internal radiotherapy delivery [42]. The half-life of ^{90}Y shows that radioactivity decays to a negligible level within 21 days after neutron bombardment, as such stability and minimal leaching of active radioisotopes during this period would be essential [12].

Cell culture studies were conducted to evaluate the suitability of the yttrium-containing phosphate microspheres for bone regeneration applications, aiming to determine their cytocompatibility and osteoconductivity. These properties are critical for fostering favourable interactions with host cells and promoting enhanced bone tissue regeneration. Phosphate-based

microspheres that possess the dual capability of enhancing bone regeneration, while also serving as carriers for radiotherapy, offer a distinct advantage over their counterparts limited solely to radiotherapy delivery. They provide a holistic therapeutic approach, addressing both cancer treatment and bone repair in a synergistic manner.

The cytocompatibility results showed that MG63 cells cultured with P40 microsphere conditioned media demonstrated the greatest levels of metabolic activity after 7 days and were comparable to that of cells cultured in standard media (SM). Cells cultured in both 30Y and 50Y media had significantly lower metabolic activity ($p < 0.001$) than those cultured in SM and P40 media at day 7. However, their relatively high activity and the significant increase in metabolic activity seen from day 2 to day 7 demonstrated their cytocompatibility. Previous *in vitro* studies of porous glass microspheres of the P40 formulation ($40\text{P}_2\text{O}_5 \cdot 16\text{CaO} \cdot 24\text{MgO} \cdot 20\text{Na}_2\text{O}$ mol%) showed that they were biocompatible according to the standard ISO 10993-5. Hossain *et al.* showed that the proliferation rate of hMSCs grown using an indirect culture method was shown to be greater than 70% of the cells grown in the SM when using an MTT assay [43].

As seen in Figure 4, P40 solid microspheres degraded faster than both the 30Y and 50Y microspheres and hence released a significantly greater amount of the glass forming ions. The simultaneous exposure and quantity of ions released from the different microsphere formulations to the cells resulted in differences in cell response. Phosphate, calcium, magnesium and sodium ions have all been shown to play vital roles within bone metabolism and homeostasis [44]. These ions are essential for various cellular functions, including signaling, energy production, and the maintenance of cellular homeostasis. Extracellular Ca^{2+} plays a key role in the regulation of osteoblastic proliferation and differentiation by influencing the expression of specific Ca^{2+} -channel isoforms on osteoblasts [45]. Enhanced cell proliferation is crucial for the initial phase of bone regeneration, where a robust population of osteoprogenitor cells is required to initiate the repair process. The increased release of ions and subsequent exposure to cells from P40 microspheres was therefore likely responsible for the increased metabolic activity observed at day 2 and 7 when compared to the 30Y and 50Y formulations.

ALP is constitutively active at low levels in all cells, but during the early stages of osteogenic differentiation its activity significantly increases [46]. It is therefore used as a marker for the detection of early osteogenic differentiation. Cells exposed to P40 ion release products had significantly greater ALP activity compared to 30Y and 50Y formulations. Similar ALP activity within cells exposed to 30Y and 50Y correlated with the ion release data in that the levels were significantly lower for the two formulations and resulted in no significant difference between them.

When cells were seeded directly on to the microspheres, both the 30Y, 50Y and parent P40 glass microspheres promoted cell growth, as seen by an increase in metabolic activity from day 2 to day 7. Cells cultured on 30Y microspheres showed initially higher cell metabolic activity at day 2. However, no statistically significant difference in metabolic activity was observed after 7 days of culture on the two yttrium-containing

formulations. Surface roughness has been shown to play a conductive role in the initial cellular adhesion and may explain the difference in metabolic activity at day 2 [47]. The durable nature of the yttrium-containing microspheres highlighted that minimal changes to the material surface integrity and a stable pH of the local microenvironment (see Figure 4F) facilitated a suitable environment for cell adhesion. The addition of ions, such as titanium and iron, is commonly employed to increase the durability of phosphate-based glasses to increase cell adhesion and provide a more stable surface to support cell proliferation and differentiation [48]. Whilst the material surface is vital for cell adhesion and colony establishment, it is not the sole determinant of subsequent biological processes, as the degradation products have the potential to influence the proliferation and differentiation of the cells [49].

Cells grown on P40, 30Y and 50Y microspheres all had increased ALP activity in comparison to TCP after 7 days of culture. The increased ALP activity of cells cultured on the microspheres suggested that microspheres provide for a more favourable surface for influencing osteoblast cell differentiation than TCP. It was likely that the phosphate, calcium, magnesium and sodium ions released from the microspheres were stimulating an early osteogenic response. Studies have established that Ca^{2+} ions are required to promote osteocalcin expression and matrix mineralisation, whilst certain concentrations of phosphate and Mg^{2+} added to cells in culture can further induce mineralisation [50]. This is particularly important for bone repair applications, as the formation of a mineralised bone matrix is essential for the restoration of bone structure and function. The lower ion release rates from the yttrium-containing microspheres could lead to a more controlled and sustained release of therapeutic ions, supporting prolonged osteogenic activity and stability in the bone microenvironment. Cells grown on TCP were not exposed to these additional ions and is likely why there was significantly lower ALP activity in these cells. To comprehensively understand the biological implications of the microspheres' stability and ion release profiles, future longer-term cell culture studies would also be beneficial. This would allow for evaluation of the impact of sustained ion release and surface integrity on bone cell activity, differentiation, and the overall mineralisation process over extended periods.

The spherical geometry of the microspheres allows for a more even distribution of cells around the biomaterial in comparison to irregular-shaped materials. This provides a more consistent microenvironment for cell growth and differentiation, crucial for studying tissue regeneration. The surface topography of biomaterials has also been shown to directly influence cellular responses including adhesion, proliferation and osteogenic differentiation [51]. Rough surfaces of native bones mineralised extracellular matrix (ECM) has been identified as an important feature that promotes adhesion and differentiation of osteoprogenitor cells to an osteogenic lineage [52]. A rough topography therefore can effectively mimic the mineralised ECM interface that cells adhere to *in vivo* when participating in bone remodelling and regeneration. The increased ALP activity seen in cells grown on the 30Y and 50Y microspheres, in comparison to the P40 microspheres, may be due to the surface roughness and topographies although this warrants further study.

The current study emphasises the prospect of yttrium containing calcium phosphate glass-ceramics as materials to facilitate bone repair. The ability to neutron activate the yttrium-containing microspheres demonstrates their capability beyond bone regeneration and may be used to deliver localised radiotherapy at the site of delivery. The novel microsphere formulations satisfy the necessary requirements for internal radiotherapy applications in that they; (i) contain high levels of radionuclide within their structure capable of delivering therapeutic radiation, and (ii) are chemically durable and resistant to physiological fluids to prevent substantially radionuclide release during period of radioactivity. Additionally, the yttrium-containing microspheres were cytocompatible and supported osteoblast-like cell growth and proliferation. Microspheres with the capacity to promote bone regeneration and following radiotherapy delivery surpass the utility of glass microspheres solely intended for radiotherapy, offering a comprehensive and integrated therapeutic strategy that addresses both oncological and regenerative needs.

Conclusions

In summary, this study successfully developed high yttrium-content phosphate-based glass-ceramic microspheres via flame spheroidisation for potential applications in bone cancer radiotherapy treatment and bone regeneration. The flame spheroidisation process yielded uniform microspheres, when sieved into their desired size range of 45 to 125 µm, and allowed for control over yttrium content, ranging from approximately 1 mol% to 39 mol%. EDX analysis confirmed the homogeneous distribution of yttrium and other elements throughout the microspheres, indicating uniform composition. XRD analysis revealed the presence of crystalline phases, indicative of glass-ceramic materials formation.

Upon addition of high yttrium content to phosphate glass, the material transitions from incorporating all the yttrium into the network to forming crystalline yttrium-rich phases, such as YPO₄, within the glass-ceramic microspheres. This resulted in improved chemical durability and resistance to degradation, crucial for internal radiotherapy applications. Ion release studies demonstrated reduced release rates of all ions from yttrium-containing microspheres compared to P40 glass microspheres. There was a significant decrease in the release rate of yttrium ions with increasing amounts incorporated into the microspheres. In vitro cytocompatibility studies revealed favourable cellular responses, supporting the potential of the yttrium-containing microspheres for bone regeneration applications.

The high yttrium content in the microspheres offers the advantage of enhanced radiation delivery per dose, potentially reducing the number of microspheres required for treatment. The ability to administer these microspheres via minimally invasive procedures further enhances their utility in internal radiotherapy applications. Additionally, the enhanced chemical durability ensures that the microspheres remain stable, preventing yttrium leaching and undesired irradiation of surrounding tissues, thereby ensuring localised and sustained therapeutic effects are delivered over the required treatment period.

Overall, the novel high yttrium-content phosphate glass-ceramic microspheres presented in this study offer a promising

dual-purpose platform for combined bone cancer radiotherapy treatment and bone regeneration. Their ability to deliver localised radiotherapy while supporting bone tissue regeneration represents a significant advancement in the field of biomaterials for oncological and regenerative medicine applications. Further in vitro and in vivo studies are warranted to explore their efficacy in preclinical and clinical settings.

AUTHOR INFORMATION

Corresponding Author

* ifty.ahmed@nottingham.ac.uk

Author Contributions

The manuscript was written through contributions of all authors. / All authors have given approval to the final version of the manuscript. B.M.: Investigation, formal analysis, visualisation, writing—original draft and writing—review and editing; A.A.: Investigation; A.Ab.: Methodology; T.I.: Methodology; R.L.: Conceptualisation and supervision; A.T.: Conceptualisation and supervision; I.A.: Conceptualisation, methodology, supervision and writing—review and editing. All authors have read and agreed to the published version of the manuscript.

ACKNOWLEDGMENT

This work was supported by the Engineering and Physical Sciences Research Council (EPSRC) Thematic Studentship Centre for Doctoral Training in Bioinspired Materials for Healthcare Applications [EP/R512321/1] through a doctoral training grant awarded to Ben Milborne. The authors would also like to acknowledge the Nanoscale and Microscale Research Centre (nmRC) at the University of Nottingham for use of the electron microscope facilities.

REFERENCES

1. Baskar, R., et al., Biological response of cancer cells to radiation treatment. *Front Mol Biosci*, 2014. 1: p. 24.
2. Garibaldi, C., et al., Recent advances in radiation oncology. *Ecancermedicalscience*, 2017. 11: p. 785.
3. Baskar, R., et al., Cancer and radiation therapy: current advances and future directions. *Int J Med Sci*, 2012. 9(3): p. 193-9.
4. Caccina, D., et al., Study of yttrium containing bioactive glasses behaviour in simulated body fluid. *J Mater Sci Mater Med*, 2006. 17(8): p. 709-16.
5. Mosconi, C., et al., Radioembolization with Yttrium-90 microspheres in hepatocellular carcinoma: Role and perspectives. *World J Hepatol*, 2015. 7(5): p. 738-52.
6. Baine, F., S. Hamzehlou, and S. Kargozar, Bioactive Glasses: Where Are We and Where Are We Going? *Journal of Functional Biomaterials*, 2018. 9(1): p. 25.
7. Molvar, C. and R. Lewandowski, Yttrium-90 Radioembolization of Hepatocellular Carcinoma-Performance, Technical Advances, and Future Concepts. *Semin Intervent Radiol*, 2015. 32(4): p. 388-97.
8. Edeline, J., et al., Yttrium-90 microsphere radioembolization for hepatocellular carcinoma. *Liver Cancer*, 2015. 4(1): p. 16-25.
9. Milborne, B.A., Abul; Layfield, Rob; Thompson, Alexander; Ahmed, Ifty The Use of Biomaterials in Internal Radiation Therapy. *Recent Progress in Materials*, 2020. 2(2).

10. Westcott, M.A., et al., The development, commercialization, and clinical context of yttrium-90 radiolabeled resin and glass microspheres. *Adv Radiat Oncol*, 2016. 1(4): p. 351-364.
11. Islam, M.T., et al., Bioactive calcium phosphate-based glasses and ceramics and their biomedical applications: A review. *J Tissue Eng*, 2017. 8: p. 2041731417719170.
12. Cacaina, D., et al., The behaviour of selected yttrium containing bioactive glass microspheres in simulated body environments. *J Mater Sci Mater Med*, 2008. 19(3): p. 1225-33.
13. Kawashita, M., et al., Preparation, structure, and in vitro chemical durability of yttrium phosphate microspheres for intra-arterial radiotherapy. *J Biomed Mater Res B Appl Biomater*, 2011. 99(1): p. 45-50.
14. Sheindlin, A., M. Kenisarin, and V. Chekhovskoi, Melting point of yttrium oxide. 1974.
15. Day, D.E., Glasses for radiotherapy, in *Bio-Glasses*, R. Baskar and K.A. Lee, Editors. 2012, John Wiley & Sons: NJ, USA. p. 203-228.
16. Barros Filho, E.C., et al. Development and evaluation of holmium doped phosphate glass microspheres for selective internal radiotherapy. in *INAC 2013: international nuclear atlantic conference*. 2013. Brazil.
17. Sene, F.F., J.R. Martinelli, and E. Okuno, Synthesis and characterization of phosphate glass microspheres for radiotherapy applications. *Journal of Non-Crystalline Solids*, 2008. 354(42): p. 4887-4893.
18. Martin, R.A., et al., Structure and thermal properties of yttrium aluminophosphate glasses. *J Phys Condens Matter*, 2008. 20(11): p. 115204.
19. Arafat, A., et al., Thermal and crystallization kinetics of yttrium-doped phosphate-based glasses. *International Journal of Applied Glass Science*, 2020. 11(1): p. 120-133.
20. Christie, J.K. and A. Tilocca, Integrating biological activity into radioisotope vectors: molecular dynamics models of yttrium-doped bioactive glasses. *Journal of Materials Chemistry*, 2012. 22(24): p. 12023-12031.
21. Islam, M.T., et al., Effect of magnesium content on bioactivity of near invert phosphate-based glasses. *International Journal of Applied Glass Science*, 2017. 8(4): p. 391-402.
22. Arafat, A., et al., Yttrium doped phosphate-based glasses: structural and degradation analyses. *Biomedical Glasses*, 2020. 6(1): p. 34-49.
23. Nuzulia, N., et al., Developing Highly Porous Glass Microspheres via a Single-Stage Flame Spheroidisation Process. *Journal of Physics: Conference Series*, 2022. 2243: p. 012005.
24. Nuzulia, N.A., et al., The Use of Microspheres for Cancer Embolization Therapy: Recent Advancements and Prospective. *ACS Biomater Sci Eng*, 2024.
25. Hadush Tesfay, A., et al., Control of Dopant Distribution in Yttrium-Doped Bioactive Glass for Selective Internal Radiotherapy Applications Using Spray Pyrolysis. *Materials (Basel)*, 2019. 12(6).
26. Ghahramani, M., et al., A Novel Way to Produce Yttrium Glass Microspheres. 2015.
27. d'Abadie, P., et al., Microspheres Used in Liver Radioembolization: From Conception to Clinical Effects. *Molecules*, 2021. 26(13).
28. Arranja, A.G., et al., Preparation and characterization of inorganic radioactive holmium-166 microspheres for internal radionuclide therapy. *Materials Science and Engineering: C*, 2020. 106: p. 110244.
29. Kawashita, M., et al., Preparation of ceramic microspheres for in situ radiotherapy of deep-seated cancer. *Biomaterials*, 2003. 24(17): p. 2955-63.
30. Christie, J.K., J. Malik, and A. Tilocca, Bioactive glasses as potential radioisotope vectors for in situ cancer therapy: investigating the structural effects of yttrium. *Physical Chemistry Chemical Physics*, 2011. 13(39): p. 17749-17755.
31. Parsons, A.J., et al., Synthesis and degradation of sodium iron phosphate glasses and their in vitro cell response. *J Biomed Mater Res A*, 2004. 71(2): p. 283-91.
32. Yue, Y., et al., Effect of Al₂O₃ on structure and properties of Al₂O₃-K₂O-P₂O₅ glasses. *Optical Materials Express*, 2018. 8(2): p. 245-258.
33. Abou Neel, E.A., W. Chrzanowski, and J.C. Knowles, Effect of increasing titanium dioxide content on bulk and surface properties of phosphate-based glasses. *Acta Biomater*, 2008. 4(3): p. 523-34.
34. Marino, A., et al., Durable phosphate glasses with lower transition temperatures. *Journal of Non-crystalline Solids - J NON-CRYST SOLIDS*, 2001. 289: p. 37-41.
35. Fu, Y. and J.K. Christie, Atomic structure and dissolution properties of yttrium-containing phosphate glasses. *International Journal of Applied Glass Science*, 2017. 8(4): p. 412-417.
36. Schaller, T. and J.F. Stebbins, The Structural Role of Lanthanum and Yttrium in Aluminosilicate Glasses: A ²⁷Al and ¹⁷O MAS NMR Study. *The Journal of Physical Chemistry B*, 1998. 102(52): p. 10690-10697.
37. Sreenivasan, H., et al., Field Strength of Network-Modifying Cation Dictates the Structure of (Na-Mg) Aluminosilicate Glasses. *Frontiers in Materials*, 2020. 7(267).
38. Malik, J. and A. Tilocca, Hydration Effects on the Structural and Vibrational Properties of Yttrium Aluminosilicate Glasses for in Situ Radiotherapy. *The Journal of Physical Chemistry B*, 2013. 117(46): p. 14518-14528.
39. Baino, F., et al., Biomedical Radioactive Glasses for Brachytherapy. *Materials*, 2021. 14(5): p. 1131.
40. Nommeots-Nomm, A., et al., A review of acellular immersion tests on bioactive glasses—influence of medium on ion release and apatite formation. *International Journal of Applied Glass Science*, 2020. 11(3): p. 537-551.
41. Christie, J.K. and A. Tilocca, Molecular dynamics simulations and structural descriptors of radioisotope glass vectors for in situ radiotherapy. *J Phys Chem B*, 2012. 116(41): p. 12614-20.
42. Hossain, K.M.Z., et al., Porous calcium phosphate glass microspheres for orthobiologic applications. *Acta Biomater*, 2018. 72: p. 396-406.
43. Hoppe, A., V. Mouriño, and A.R. Boccaccini, Therapeutic inorganic ions in bioactive glasses to enhance bone formation and beyond. *Biomaterials Science*, 2013. 1(3): p. 254-256.
44. Maeno, S., et al., The effect of calcium ion concentration on osteoblast viability, proliferation and differentiation in monolayer and 3D culture. *Biomaterials*, 2005. 26(23): p. 4847-4855.
45. Patel, U., et al., In vitro cellular testing of strontium/calcium substituted phosphate glass discs and microspheres shows potential for bone regeneration. *J Tissue Eng Regen Med*, 2019. 13(3): p. 396-405.
46. Zareidoost, A., et al., The relationship of surface roughness and cell response of chemical surface modification of titanium. *Journal of materials science. Materials in medicine*, 2012. 23(6): p. 1479-1488.
47. Lakhkar, N.J., et al., Titanium phosphate glass microspheres for bone tissue engineering. *Acta Biomater*, 2012. 8(11): p. 4181-90.
48. De Melo, N., et al., Tailoring Pyro- and Orthophosphate Species to Enhance Stem Cell Adhesion to Phosphate Glasses. *International Journal of Molecular Sciences*, 2021. 22(2): p. 837.
49. Yoshizawa, S., et al., Magnesium ion stimulation of bone marrow stromal cells enhances osteogenic activity, simulating the effect of magnesium alloy degradation. *Acta Biomaterialia*, 2014. 10(6): p. 2834-2842.
50. Zhang, J., et al., Topography of calcium phosphate ceramics regulates primary cilia length and TGF receptor recruitment associated with osteogenesis. *Acta Biomaterialia*, 2017. 57: p. 487-497.
51. Du, Y., et al., Hierarchically designed bone scaffolds: From internal cues to external stimuli. *Biomaterials*, 2019. 218: p. 119334-119334.

for Table of Contents use only

